Physics of the Solid State, Vol. 45, No. 4, 2003, pp. 762–767. Translated from Fizika Tverdogo Tela, Vol. 45, No. 4, 2003, pp. 725–729.
Original Russian Text Copyright © 2003 by Kul'bachinskiĭ, Lunin, Rogozin, Golikov, Kytin, Zvonkov, Nekorkin, Filatov, de Visser.

Quantum Hall Effect–Insulator Transition in the InAs/GaAs System with Quantum Dots

V. A. Kul'bachinskiĭ*, R. A. Lunin*, V. A. Rogozin*, A. V. Golikov*, V. G. Kytin*, B. N. Zvonkov*, S. M. Nekorkin*, D. O. Filatov*, and A. de Visser**

** Moscow State University, Vorob'evy gory, Moscow, 119899 Russia*

*** Van der Waals–Zeeman Institute, University of Amsterdam, 1018 XE Amsterdam, The Netherlands*

Received April 9, 2002; in final form, August 16, 2002

Abstract—The InAs/GaAs structures consisting of quantum-dot layers with electronic properties typical of two-dimensional systems are investigated. It is found that, at a low concentration of charge carriers, the variable-range-hopping conductivity is observed at low temperatures. The localization length corresponds to characteristic quantum-dot cluster sizes determined using atomic-force microscopy (AFM). The quantum Hall effect–insulator transition induced by a magnetic field occurs in InAs/GaAs quantum-dot layers with metallic conductivity. The resistivities at the transition point exceed the resistivities characteristic of electrons in heterostructures and quantum wells. This can be explained by the large-scale fluctuations of the potential and, hence, the electron density. *© 2003 MAIK "Nauka/Interperiodica".*

1. INTRODUCTION

The quantum Hall effect–insulator transition is a fundamental phenomenon in the physics of two-dimensional systems [1–5]. At temperatures close to zero, two-dimensional electrons in a magnetic field perpendicular to the plane of a disordered two-dimensional gas can occur in three stable states: (i) an insulating state when the diagonal elements of the conductivity tensor σ_{xx} tends to zero and the diagonal elements of the resistivity tensor ρ_{xx} tends to infinity at $T \longrightarrow 0$; (ii) a Hall liquid state when $\sigma_{xx} \longrightarrow 0$, $\rho_{xx} \longrightarrow 0$, and the Hall component σ_{xy} of the conductivity tensor is quantized, i.e., $\sigma_{xy} = (e^2/h)s_{xy}$, where s_{xy} is an integer (the integer quantum Hall effect) or a rational fraction (the fractional quantum Hall effect); and (iii) a Hall insulating state when $\sigma_{xx} \longrightarrow 0$ and $\sigma_{xy} \longrightarrow 0$ at $T \longrightarrow 0$ but $\sigma_{xy} \propto (\sigma_{xx}^2)$, so that $\rho_{xy} \longrightarrow \rho_{xy}(0) \approx B/ne$, where n is the two-dimensional electron density, B is the magnetic field induction, and e is the elementary charge. In general, the state of a two-dimensional system is determined primarily by the magnetic field induction and the degree of disordering in the system [1]. According to the phase diagram proposed by Kivelson *et al.* [1] for a two-dimensional system, an increase in the magnetic field induction can lead to variations in the conducting properties, i.e., to metal–insulator transitions, in slightly disordered systems.

The metal–insulator transitions induced by magnetic fields have been studied to sufficient detail in two-dimensional systems with a high degree of ordering, for example, in heterojunctions and quantum wells [4–6]. However, the specific features of this phenomenon in two-dimensional systems with a high degree of disordering call for further investigation. In particular, it remains unclear how fluctuations of the potential and the electron density affect the quantum Hall–insulator transition in a two-dimensional system in the vicinity of the localization threshold.

A layer of quantum dots with a high surface density can be treated as a specific two-dimensional system. In such a structure, the wave functions of electrons can be delocalized through the overlap of the wave functions of electrons localized in adjacent quantum dots. The degree of disordering depends on the growth conditions of the structure. Actually, one way to decrease the spread in the positions and sizes of quantum dots is to grow these dots on vicinal surfaces of semiconductors [7, 8].

Structures with quantum-dot layers are new objects that are particularly suitable for investigation of strong and weak localizations of charge carriers, hoping conductivity, quantum Hall effect, and metal–insulator transitions in magnetic fields. Elucidation of the specific features of charge carrier transfer in InAs/GaAs quantum-dot layers is of considerable practical importance, because these systems are widely used in manufacturing semiconductor lasers [9], single-electron transistors, and memory elements [10] of the new generation.

In this work, we investigated the specific features of the transport properties and the quantum Hall effect–insulator transition in InAs quantum-dot layers in the GaAs matrix.

2. SAMPLE PREPARATION AND EXPERIMENTAL TECHNIQUE

Samples containing InAs quantum-dot layers were grown through metalloorganic chemical vapor deposition under atmospheric pressure (the so-called MOC hydride epitaxy) at temperatures of 600–650°C. The growth was performed on a GaAs(001) semi-insulating substrate misoriented by 3° in the [110] direction with respect to the (001) plane. This substrate (referred to as the vicinal substrate) is characterized by the formation of steps whose height is equal to the thickness of one GaAs monolayer and width depends on the misorientation angle. The use of the vicinal surface for the dot growth makes it possible to obtain dots with a more uniform size distribution [7, 8]. In our experiments, we examined three samples. The structure of the studied samples consisted of 10 (samples *1*, *3*) or 12 (sample *2*) stacks, each containing a 0.1-μm-thick GaAs layer and an InAs quantum-dot layer. This structure was capped with a GaAs cladding layer 0.1 μm thick. We measured the sheet conductivity. In *n*-type samples *1* and *3*, the electron concentrations per layer of quantum dots were equal to 4.0×10^{10} and 1.9×10^{11} cm^{-2} and the electron mobilities were 1000 and 5500 cm^2/Vs, respectively. In *p*-type sample *2*, we additionally prepared a δ-C doping layer, which was separated from the quantum-dot layer by a 5-nm-thick GaAs undoped spacer. In this sample, the hole concentration per layer of quantum dots was 2.7×10^{11} cm^{-2} and the hole mobility was approximately equal to 100 cm^2/Vs. The charge carrier concentrations were determined from the Hall effect at a temperature of 4.2 K. A schematic drawing of the structure of a *p*-type sample is given in Fig. 1.

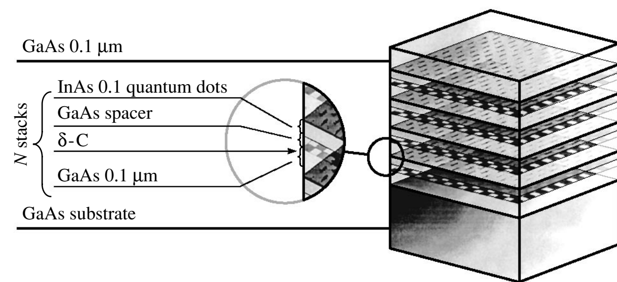

Fig. 1. Schematic drawing of the structure of the studied samples.

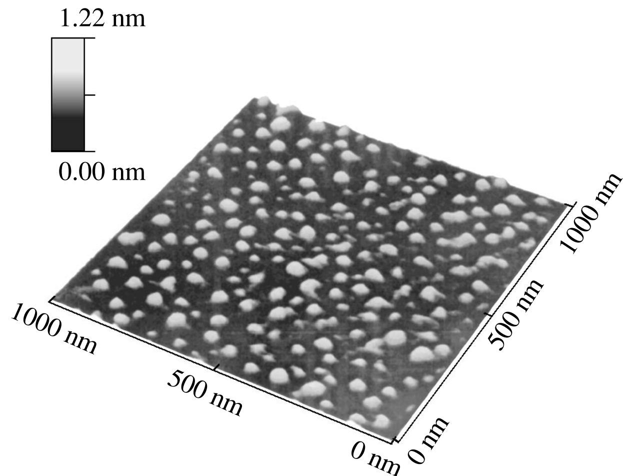

Fig. 2. AFM image of a quantum-dot layer after removal of a cladding layer by selective etching.

The morphology of the quantum-dot layer was investigated using a TopoMetrix® TMX-2100 Accurex^{TM} atomic-force microscope (AFM) operating in a contact mode in air. In order to visualize the quantum dots, the cladding layer was subjected to selective etching in a mixture of a 0.8 *M* $K_3[Fe(CN)_6]$ solution in 0.3 *M* KOH with water and glycerol in the ratio 1 : 5 : 2. The technique of AFM observations was described in detail in [11]. Figure 2 displays the AFM image of the surface of a quantum-dot layer after etching. Quantum dots with lateral sizes of ~50 nm, a height of ~1.2 nm, and a surface density $N_S \approx 2 \times 10^{10}$ cm^{-2} are clearly distinguished in the AFM image. A histogram of the distribution of quantum dots over sizes L at the base is depicted in Fig. 3a. The probability density of the radial distribution $W(r)$ of quantum-dot clusters is presented in Fig. 3b. The probability $dP(r, \Delta r)$ of finding a cluster in the ring $(r, r + \Delta r)$ is defined by the equation $dP(r, \Delta r) = 2\pi r W(r)\Delta r$.

The magnetotransport measurements were performed using a standard method in the temperature range 1.35–4.2 K at a current of 1–2 μA along the quantum-dot layers. The Hall resistivity $\rho_{xy}(B)$ and the magnetoresistivity $\rho_{xx}(B)$ were measured in a magnetic field perpendicular to the quantum-dot layers, i.e., perpendicular to the current flow (hereafter, all the experimental resistivities will be given per layer of quantum dots). A magnetic field up to 10 T was induced by a superconducting solenoid. Stronger magnetic fields (up to 40 T) were generated at the University of Amsterdam with the use of the pulse method at a freely decaying current. This provided a means for the generation of quasi-stationary magnetic fields with a pulse duration of 1–2 s. The samples were placed in liquid helium in order to prevent their overheating. The temperature was varied through evacuation of helium vapors.

3. RESULTS AND DISCUSSION

3.1. Strong Localization of Charge Carriers

In the structures under investigation, the quantum dots are filled with charge carriers. At a sufficiently high concentration, the quantum dots can form two-dimensional electrons that exhibit the Shubnikov–de Haas and quantum Hall effects [12–15]. A decrease in the charge carrier concentration does not change the two-dimensional character of conductivity but can result in a crossover to hopping conductivity. Figure 4a shows the temperature dependences of the resistivity

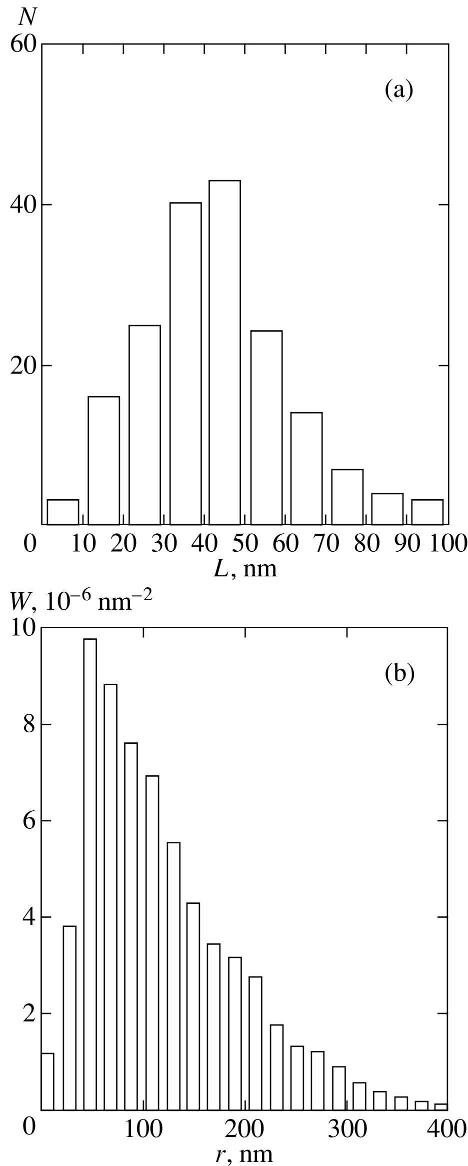

Fig. 3. (a) Distribution of the number of quantum dots N over sizes L at the base and (b) the probability density of the radial distribution $W(r)$ of quantum-dot clusters according to the AFM data.

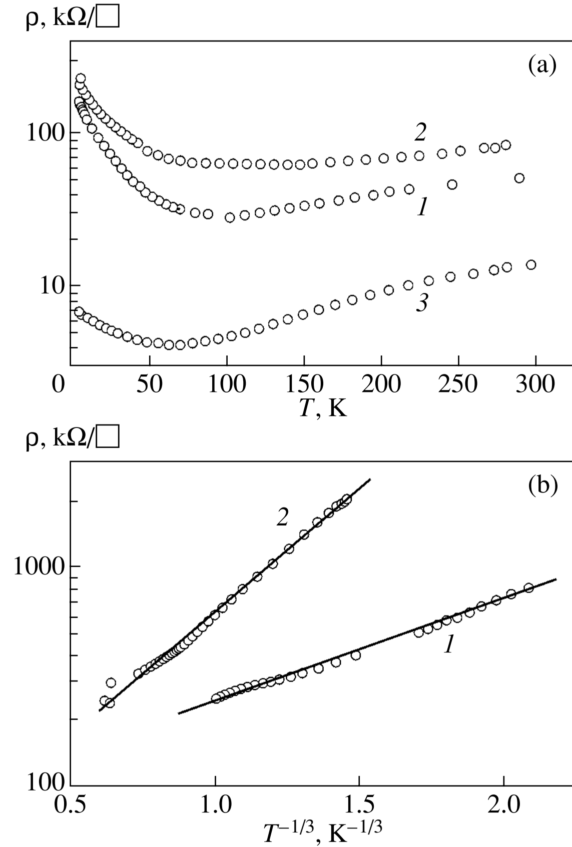

Fig. 4. (a) Temperature dependences of the resistivity (resistance per square) for (*1*) *n*-type sample *1*, (*2*) *n*-type sample *3*, and (*3*) *p*-type sample *2*. (b) Low-temperature portions of the temperature dependences of the resistivity for (*1*) sample *1* and (*2*) sample *2*.

for two *n*-type samples and one *p*-type sample. It can be seen from this figure that, in all cases, the resistivity passes through a minimum. This indicates that the resistivity of the studied samples at high temperatures increases with increasing temperature (as is the case in metals), whereas the localization effects become pronounced at the liquid-helium temperature. At low temperatures, samples *1* and *2* possess variable-range-hopping conductivity. In this temperature range, the resistivity of samples *1* and *2* obeys the Mott law for two-dimensional hopping conductivity and can be represented by the relationship $\rho = \rho_0 \exp\{(T_0/T)^{1/3}\}$ [16]. The low-temperature portions of the temperature dependences of the resistivity for these samples in the corresponding coordinates are depicted in Fig. 4b. The parameter T_0 is related to the density of states at the Fermi level N_{E_F} and the localization length a through the expression $T_0 = C(N_{E_F} a^2)^{-1}$, where $C = 13.8$ is the numerical coefficient [16]. For sample *2*, we have $T_0 \approx$ 17 K; hence, it follows that, the localization length a calculated from the above expression is approximately equal to 80 nm. This value approximately corresponds to the probability density $W(r)$ of the radial distribution of quantum-dot clusters at the maximum (Fig. 3b). Consequently, as the temperature decreases, the charge carriers are localized not in single quantum dots but within an extended potential relief associated with quantum-dot clusters.

For sample *3* with a sufficiently high electron concentration, the temperature dependence of the resistivity in the low-temperature range is consistent with the quantum corrections to the two-dimensional conductivity [17]; i.e., it can be rectified in the R–ln$T$ coordinates. Moreover, the negative magnetoresistivity is observed

in weak magnetic fields. This also corresponds to a weak two-dimensional localization of electrons.

Figure 5 shows the dependences of the magnetoresistivity $\rho_{xx}(B)$ of the studied samples at different temperatures. It should be noted that the initial resistivities of samples *1* and *2* substantially exceed the value of $h/e^2 \approx 25.8$ kΩ per square (where h is the Planck constant and e is the elementary charge), which is treated as a conventional boundary between the metallic and dielectric states. As the magnetic field increases, the resistivity $\rho_{xx}(B)$ passes through a minimum. The nature of this minimum will be discussed below. The sign of the derivative $d\rho_{xx}/dT$ is considered to be the main criterion for metallic properties of a system ($\{d\rho_{xx}/dT\} > 0$ for a metal and $\{d\rho_{xx}/dT\} < 0$ for an insulator) [3]. For samples *1* and *2*, the negative derivative $d\rho_{xx}/dT < 0$ takes place over the entire range of magnetic fields. This result confirms the following inference drawn above from analyzing the temperature dependence of the resistivity without a magnetic field: samples *1* and *2* are characterized by a strong localization of charge carriers. The minima observed in the resistivity are associated with the change in both the localization length of the wave function of charge carriers and the density of states at the Fermi level under the effect of a magnetic field. In weak magnetic fields, the localization length of charge carriers increases, because the magnetic field suppresses interference of electron waves that experience different sequences of scattering events in the course of tunneling [18]. As was shown by Raikh [19], the density of states at the Fermi level also increases. These two factors are responsible for the negative magnetoresistivity. Strong magnetic fields generate an additional localizing potential, which leads to a decrease in the localization length of the wave function [16]. An increase in the magnetic field brings about a decrease in the density of states at the Fermi level at a filling factor of less than unity due to a shift in the maximum of the density of states toward the high-energy range. As a result, there arises positive magnetoresistivity in strong magnetic fields. The crossover from the negative to positive magnetoresistivity is observed in magnetic fields for which the filling factor is two [4]. For samples *1* and *2*, the magnetic fields corresponding to this crossover are approximately equal to 2 and 12 T, respectively.

Making allowance for the contraction of the electron wave function in the magnetic field, we obtain the following relationship between the resistivity ρ and the magnetic field B: $\rho = \rho_0\exp(B^{1/2})$ [16]. The inclusion of the decrease in the density of states should lead to a stronger dependence. In our case, the magnetoresistivity in strong fields can be adequately described by the expression $\rho = \rho_0\exp(B)$ (Fig. 5). Note also that the resistivities of samples *1* and *2* remain larger than h/e^2 over the entire range of magnetic fields.

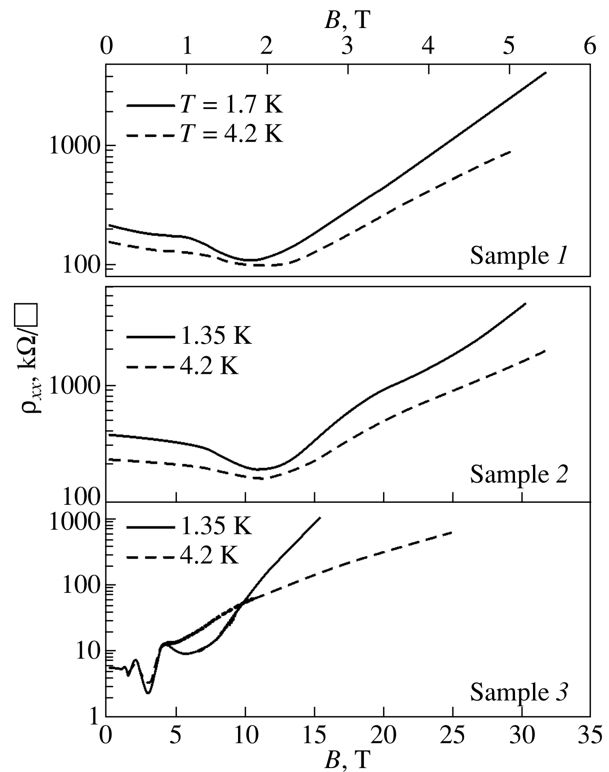

Fig. 5. Dependences of the magnetoresistivity ρ_{xx} (in kΩ per square) on the magnetic field for samples *1*–*3* at two temperatures.

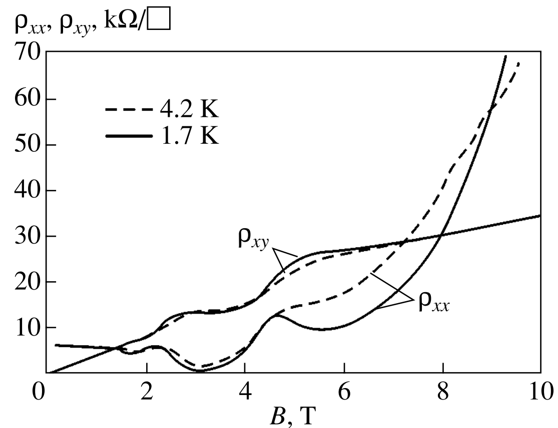

Fig. 6. Dependences of the magnetoresistivity ρ_{xx} and the Hall resistivity ρ_{xy} on the magnetic field for sample *3* at two temperatures.

3.2. The Quantum Hall Effect–Insulator Transition

Sample *3* with a relatively high electron concentration is characterized by the Shubnikov–de Haas effect, the quantum Hall effect, and the intersection of the field dependences of the magnetoresistivity measured at different temperatures (Fig. 6). At the intersection points, the derivative $d\rho_{xx}/dT$ changes sign and the quantum

Hall effect–insulator transition occurs. The positive derivative $d\rho_{xx}/dT > 0$ and a plateau in the dependences of the Hall resistivity ρ_{xy} on the magnetic field are observed in approximately the same fields. These plateaus correspond to filling factors of two and unity. Note that the quantum Hall plateau is retained after the intersection of the field dependences of the magnetoresistivity measured at two temperatures. On this basis, the phase formed upon transition was called the quantum Hall insulator [20]. The observed slope of the plateau in our case can be explained by relatively high temperatures of the measurements.

According to the existing theories of the quantum Hall effect–insulator transition [1, 5, 21], the resistivity ρ_{xx} at the transition point should be equal to h/e^2. However, the resistivity ρ_{xx} for sample *3* upon transition at $B \approx 9$ T from the quantum Hall state with a filling factor of unity to the insulating state with a zero filling factor is nearly twice as large as the value of h/e^2. This discrepancy can be explained in terms of the specific features of the two-dimensional system under consideration. In a quantum-dot layer, the overlap of the wave functions of electrons localized in different dots gives rise to two-dimensional electrons. In this case, the distances between quantum dots and their sizes are distributed in a random manner. As a result, the density of two-dimensional electrons in the layer fluctuates on a typical scale of variation in the size of quantum-dot clusters (Fig. 3b). Since the characteristic size of the electron wave function in a quantizing magnetic field is of the order of the magnetic length $l = (\hbar/eB)^{1/2} \approx 28$ nm (at the magnetic field induction $B = 1$ T), which is less than the cluster size, the energy at the Landau level also fluctuates in space. In the sample, the current predominantly flows through regions that have the highest concentrations of charge carriers and form a network of conducting channels. The effective length of the conducting channels can be considerably larger and their width can be appreciably smaller than those for a spatially homogeneous two-dimensional system. As a consequence, the resistivity of the structure in the quantum Hall regime can substantially exceed the maximum resistivity of a two-dimensional metal (h/e^2), even though the temperature dependence of the resistivity exhibits a metallic behavior.

4. CONCLUSIONS

Thus, it was demonstrated that, in InAs/GaAs structures with quantum-dot layers, the wave functions of charge carriers localized in adjacent quantum dots overlap at low temperatures. As a result, strongly localized two-dimensional charge carriers are generated and variable-range-hopping conductivity is observed at low temperatures. The localization length is approximately equal to 80 nm and agrees well with the characteristic quantum-dot cluster sizes determined from the AFM data.

At a high concentration of charge carriers, the temperature dependence of the resistivity and the negative magnetoresistivity in weak magnetic fields correspond to a weak two-dimensional localization regime. The Shubnikov–de Haas and quantum Hall effects are observed in stronger magnetic fields. The quantum Hall effect–insulator transition occurs in strong magnetic fields. It was found that the two-dimensional conductivity in the quantum Hall state at a filling factor of unity is less than the minimum metallic conductivity. In this case, the temperature dependence of the resistivity of the system exhibits metallic behavior. These findings can be explained by the strong spatial inhomogeneity of the system, in which the current passes through a network of channels formed by regions with the highest concentration of two-dimensional electrons.

ACKNOWLEDGMENTS

This work was supported by the Russian Foundation for Basic Research, project nos. 00-02-17493 and 01-02-16441. The AFM measurements were performed at the Research and Educational Center for Scanning Probe Microscopy (Nizhniĭ Novgorod State University) and were supported by the Russian– American Program "Basic Research and Higher Education" (BRHE) of the Ministry of Education of the Russian Federation and the American Civilian Research and Development Foundation for the Independent States of the Former Soviet Union (CRDF), project no. REC-001.

REFERENCES

1. S. Kivelson, D.-H. Lee, and S.-C. Zhang, Phys. Rev. B **46**, 2223 (1992).
2. E. Shimshoni, Phys. Rev. B **60**, 10691 (1999).
3. G. H. Kim, J. T. Nicholls, S. I. Khondaker, *et al.*, Phys. Rev. B **61**, 10910 (2000).
4. H. W. Jiang, C. E. Johnson, and K. L. Wang, Phys. Rev. B **46**, 12830 (1992).
5. D. Shahar, D. C. Tsui, and J. E. Cunninggham, Phys. Rev. B **52**, R14372 (1995).
6. T. Wang, K. P. Clark, G. F. Spencer, *et al.*, Phys. Rev. Lett. **72**, 709 (1994).
7. M. Kitamura, M. Nishioka, J. Oshino, and Y. Arakawa, Appl. Phys. Lett. **63**, 439 (1996).
8. V. G. Talalaev, B. V. Novikov, S. Yu. Verbin, *et al.*, Fiz. Tekh. Poluprovodn. (St. Petersburg) **34**, 467 (2000) [Semiconductors **34**, 453 (2000)].
9. F. Schafer, J. P. Reithmaier, and A. Forchel, Appl. Phys. Lett. **74**, 2915 (1999).
10. P. Recher, E. V. Sukhorukov, and D. Loss, Phys. Rev. Lett. **85**, 1962 (2000).
11. I. A. Karpovich, N. V. Baidus, B. N. Zvonkov, *et al.*, Phys. Low-Dimens. Semicond. Struct. **3/4**, 341 (2001).
12. V. A. Kulbachinskii, V. G. Kytin, R. A. Lunin, *et al.*, Microelectron. Eng. **43–44**, 107 (1998).

13. V. A. Kul'bachinskiĭ, V. G. Kytin, R. A. Lunin, *et al.*, Vestn. Mosk. Univ., Ser. 3: Fiz., Astron., No. 5, 53 (1998).
14. V. A. Kulbachinskii, V. G. Kytin, R. A. Lunin, *et al.*, Physica B (Amsterdam) **266**, 185 (1999).
15. V. A. Kul'bachinskiĭ, V. G. Kytin, R. A. Lunin, *et al.*, Fiz. Tekh. Poluprovodn. (St. Petersburg) **33**, 316 (1999) [Semiconductors **33**, 318 (1999)].
16. B. I. Shklovskiĭ and A. L. Éfros, *Electronic Properties of Doped Semiconductors* (Nauka, Moscow, 1979; Springer, New York, 1984).
17. T. A. Polyanskaya and Yu. V. Shmartsev, Fiz. Tekh. Poluprovodn. (Leningrad) **23** (1), 3 (1989) [Sov. Phys. Semicond. **23**, 1 (1989)].
18. V. N. Nguen, B. Z. Spivak, and B. I. Shklovskiĭ, Pis'ma Zh. Éksp. Teor. Fiz. **41** (1), 35 (1985) [JETP Lett. **41**, 42 (1985)].
19. M. E. Raikh, Solid State Commun. **75**, 935 (1990).
20. M. Hilke, D. Shahar, S. H. Song, *et al.*, Nature **395**, 675 (1998).
21. H. L. Zhao, B. Z. Spivak, M. P. Gelfand, and S. Feng, Phys. Rev. B **44**, 10760 (1991).

Translated by O. Borovik-Romanova